Brain Pathology ISSN 1015–6305

RESEARCH ARTICLE

Fatal familial insomnia: mitochondrial and protein synthesis machinery decline in the mediodorsal thalamus

Margalida A. Frau-Méndez[1]; Iván Fernández-Vega[2]; Belén Ansoleaga[1]; Rosa Blanco Tech[1,3]; Margarita Carmona Tech[1,3]; Jose Antonio del Rio[3,4]; Inga Zerr[5]; Franc Llorens[5]; Juan José Zarranz[6]; Isidro Ferrer[1,3]

[1] Institute of Neuropathology, Bellvitge University Hospital, University of Barcelona, Bellvitge Biomedical Research Institute (IDIBELL), Hospitalet de Llobregat, Spain.
[2] Department of Neuropathology, Pathology Department, University Hospital Araba, Álava, Brain Bank Araba University Hospital, Basque Biobank for Research (O+eHun), Spain.
[3] Department of Neuropathology, Biomedical Research Center of Neurodegenerative Diseases (CIBERNED), Spain.
[4] Department of Cell Biology, Molecular and Cellular Neurobiotechnology, Institute of Bioengineering of Catalonia (IBEC), Parc Científic de Barcelona, University of Barcelona, Barcelona, Spain.
[5] Department of Neurology, Clinical Dementia Center, University Medical School, Georg-August University and German Center for Neurodegenerative Diseases (DZNE), Göttingen, Germany.
[6] Neurology Department, University Hospital Cruces, University of the Basque Country, Bizkaia, Spain.

Keywords
fatal familial insomnia, mitochondria, mitochondrial respiratory chain, nucleolus, protein synthesis, ribosome.

Corresponding author:
Isidro Ferrer, MD, PhD, Institute of Neuropathology, Service of Pathologic Anatomy, Bellvitge University Hospital, carrer Feixa Llarga s/n, 08907 Hospitalet de Llobregat, Spain (E-mail: *8082ifa@gmail.com*)

Received 6 January 2016
Accepted 16 May 2016
Published Online Article Accepted 24 June 2016

Compliance with ethical standards
No relevant data.

The authors declare that they have no conflicts of interest.

doi:10.1111/bpa.12408

Abstract

The expression of subunits of mitochondrial respiratory complexes and components of the protein synthesis machinery from the nucleolus to the ribosome was analyzed in the mediodorsal thalamus in seven cases of fatal familial insomnia (FFI) compared with age-matched controls. NDUFB8 (complex I subunit), SDHB (complex II subunit), UQCRC2 (complex III subunit), COX2 (complex IV subunit), and ATP50 (complex V subunit) expression levels, as revealed by western blotting, were reduced in FFI. Voltage-dependent anion channel (VDAC) and ATP5H were also reduced due to the marked depopulation of neurons. In contrast, a marked increase in superoxide dismutase 2 (SOD2) was found in reactive astrocytes thus suggesting that astrocytes are key factors in oxidative stress responses. The histone-binding chaperones nucleolin and nucleoplasmin 3, and histone H3 di-methylated K9 were markedly reduced together with a decrease in the expression of protein transcription elongation factor eEF1A. These findings show severe impairment in the expression of crucial components of mitochondrial function and protein synthesis in parallel with neuron loss in mediodorsal thalamus at terminal stages of FFI. Therapeutic measures must be taken long before the appearance of clinical symptoms to prevent the devastating effects of FFI.

INTRODUCTION

Prion protein is encoded by *PRNP* located on the short arm of chromosome 20 in humans. The second exon of *PRNP* encodes a protein of 253 amino acids that is truncated post-translationally to remove 22 amino acids at the amino-terminal and 23 amino acids at the carboxyl-terminal, being replaced at this site by the addition of a glycosylphosphatidylinositol (GPI) anchor. Additional putative glycosylation in two asparagine sites gives rise to three isoforms, fully di-glycosylated, mono-glycosylate, and nonglycosylated prion protein (3). Mutations in *PRNP* are causative of genetic prion diseases, some of which are manifested as familial Creutzfeldt-Jakob disease (CJD), the phenotype of which depends on the site of *PRNP* mutation and also on the polymorphism of codon 129 in *PRNP* (3).

Fatal familial insomnia (FFI) is an autosomal dominant prion disease caused by a D178N mutation in *PRNP* in combination with methionine (Met) at codon 129 in the mutated allele of the same gene (D178N-129M haplotype) (15, 23–26, 30). Homozygosity, either methionine–methionine or valine–valine, at codon 129 in the normal allele of *PRNP* results in acceleration of clinical symptoms and shorter duration of the disease (5, 13, 28).

Clinically, FFI is principally manifested as sleep disturbances with insomnia, sleep fragmentation, and altered arousal and

dreaming, accompanied by autonomic disturbances including increased salivation and sweating, tachycardia, hypertension, and impotence, as well as spontaneous and evoked myoclonus, among other neurological symptoms (5, 12, 14, 17, 20, 21, 28, 37).

Clinical symptoms reflect major atrophy of the anterior ventral and mediodorsal limbic nuclei of the thalamus that extends to the pulvinar, ventral anterior and ventral medial thalamic nuclei with disease progression. The inferior olives are the other major targets in FFI. Severe neuron loss and astrogliosis without spongiform change in these regions, in the context of familial disease, are the neuropathological characteristics of FFI. Moderate astrogliosis without neuron loss is common in the periaqueductal gray matter and hypothalamus. Involvement of the inner temporal cortex, including CA1 region of the hippocampus, cingular cortex and other areas of the neocortex, is variable and depends on the duration of the disease, which in turn largely depends on the codon 129 polymorphism (14, 21, 22, 26, 28).

The deposition of abnormal prion protein (PrP^{Sc}) varies from one region to another in FFI. Immunohistochemistry usually shows small granular deposits in the temporal neocortex in cases with relatively long duration, whereas PrP^{Sc} deposition in thalamus is very scanty, if present. However, western blotting identifies a particular pattern characterized by a weak band of proteinase-resistant non-glycosylated PrP^{Sc} at 19 kDa (type 2 PrP) and relatively strong bands of mono-glycosylated and di-glycosylated PrP^{Sc} which disappear following PNGase digestion, giving rise to a robust non-glycosylated band (14, 28–30).

Recent studies of gene expression profiling have shown altered gene expression in the thalamus in FFI cases when compared with controls. The main changes correspond to the following biological processes: transcription, regulation of transcription, protein biosynthesis, protein folding, protein transport, RNA splicing, electron transport chain, oxidative phosphorylation, energy metabolism, transport, and oxidation reduction (36). Proteomics methods have also been employed to assess altered protein profiles in FFI. Proteins involved in protein export and oxidative phosphorylation, as well as proteins involved in other neurodegenerative diseases as Alzheimer's disease and Parkinson's disease have been identified in the cortex and cerebellum (34). Unfortunately, the thalamus was not examined.

Because of the limited knowledge about altered metabolic pathways in FFI, the present study was designed to learn about alterations of two major complex pathways, one regulating energy metabolism, and particularly mitochondrial function, and the other protein synthesis. The study was performed on postmortem samples of the thalamus of seven well-characterized cases of FFI which were analyzed using combined qRT-PCR (quantitative real-time polymerase chain reaction), western blotting and immunohistochemistry.

MATERIALS AND METHODS

Human samples

All the cases were from the Basque Country in the north of Spain where FFI has a relative high incidence due to a founder effect in a historically small rural community with not uncommon endogamy (31). This study was focused on the mediodorsal thalamus from seven FFI cases and seven controls (Table 1).

Table 1. Summary of the main clinical and pathologic features of cases used in this study. Abbreviations: PMD = postmortem delay; C = control; FFI = fatal familial insomnia; RIN = RNA integrity number; Thal = mediodorsal thalamus.

Case	Sex	Age	PMD	Neuropathology	RIN Thal
1	M	67	14 h 40 minutes	C	6
2	M	61	4 h 30 minutes	C	7.2
3	M	59	4 h 15 minutes	C	6.6
4	W	66	12 h 10 minutes	C	6.7
5	M	76	4 h 15 minutes	C	6
6	M	81	11 h 40 minutes	C	6
7	M	57	5 h	C	6.9
8	M	53	12 h 10 minutes	FFI	7.9
9	M	56	22 h 50 minutes	FFI	5.3
10	M	36	17 h 30 minutes	FFI	6.4
11	M	70	15 h 30 minutes	FFI	-
12	M	50	12 h 30 minutes	FFI	6.8
13	M	47	3 h 30 minutes	FFI	8.2
14	M	54	9 h 50 minutes	FFI	7.5

All FFI cases were males, had the mutation D178N and were Met/Met homozygous at the codon 129 of *PRNP*. The most common age at onset was between 47 and 57 years (five cases) with the exception of one young person aged 36 and one old individual aged 70. The duration of the disease was between 6 and 16 months independently of the age at onset.

Brain tissue was obtained from the Brain Bank of the Araba University Hospital and Basque Biobank for Research (O + eHun) and the Institute of Neuropathology Biobank following the guidelines of the Spanish legislation on this matter and the approval of the local ethics committees. The postmortem interval between death and tissue processing was between 4 h 15 minutes and 22 h 50 minutes. One hemisphere was immediately cut in coronal sections, 1 cm thick, and selected areas of the encephalon were rapidly dissected, frozen on metal plates over dry ice, placed in individual air-tight plastic bags, numbered with water-resistant ink and stored at −80°C until use. The other hemisphere was fixed by immersion in 4% buffered formalin for 3 weeks. Neuropathological examination in all cases was routinely performed on 20 selected dewaxed paraffin sections comprising different regions of the cerebral cortex, diencephalon, thalamus, brain stem, and cerebellum which were stained with haematoxylin and eosin, Nissl staining, and for immunohistochemistry to microglia using antibodies Iba1 and CD68, glial fibrillary acidic protein (GFAP), β-amyloid, phosphorylated tau (clone AT8), PrP (using the 3F4 antibody without and with pretreatment with proteinase K), α-synuclein, TDP-43, ubiquitin and p62. FFI cases were pretreated with formic acid. Age-matched control cases had not suffered from neurologic, psychiatric, or metabolic diseases (including metabolic syndrome), and did not have abnormalities in the neuropathological examination excepting sporadic Alzheimer's disease-related pathology stages I-II/0 of Braak and Braak.

RNA extraction

RNA was obtained from about 100 mg of the dorsomedial thalamus of FFI cases and controls using RNeasy Lipid Tissue Mini Kit (Qiagen, Hilden, GE) following the protocol provided by the

supplier. All samples were treated with RNase-free DNase Set (Qiagen) for 15 minutes to eliminate genomic DNA contamination. The concentration of each sample was measured using a NanoDrop 2000 spectrophotometer (Thermo Scientific, Waltham, MA, USA) at 340 nm. RNA integrity was assessed with the RNA Integrity Number (RIN value) determined with the Agilent 2100 Bioanalyzer (Agilent, Santa Clara, CA, USA) (33). RIN values were similar in control and FFI cases (Table 1).

Retro-transcription reaction

Retro-transcription reaction of RNA samples was carried out with the High-Capacity cDNA Archive kit (Applied Biosystems, Foster City, CA, USA) using 1000 ng of RNA for each sample following the protocol provided by the supplier using a Gene Amp 9700 PCR System thermos-cycler (Applied Biosystems). RNA samples without reverse transcriptase were processed in parallel as controls of the reaction. No amplifications were obtained in any cases.

Real-time polymerase chain reaction)

Quantitative RT-PCR assays were performed in duplicate on cDNA samples obtained from the retro-transcription reaction diluted 1:20 in 384-well optical plates (Kisker Biotech, Steinfurt, GE) using the ABI Prism 7900 HT Sequence Detection System (Applied Biosystems). The reactions were carried out using 20xTaqMan Gene Expression Assays for genes involved in protein synthesis, energetic metabolism and purine metabolism, and 2xTaqMan Universal PCR Master Mix (Applied Biosystems). TaqMan probes used in the study are shown in Table 2. The reactions were conducted with the following parameters: 50°C for 2 minutes, 95°C for 10 minutes, 40 cycles at 95°C for 15 s and 60°C for 1 minute. The data were captured using the Sequence Detection Software (SDS version 2.2, Applied Biosystems). Threshold cycle (CT) data for each sample were analyzed with the Livak Method or double delta CT (ΔΔCT) method (19). First, delta CT (ΔCT) values were calculated as the normalized CT values for each target gene in relation to the endogenous control X-prolyl aminopeptidase P1 (*XPNPEP1*) used as housekeeping gene (9). Second, ΔΔCT values were obtained from the ΔCT of each sample minus the mean ΔCT of control samples. The fold change was determined using the equation $2^{-\Delta\Delta CT}$. Mean fold-change values for every region between FFI cases and controls were analyzed with the Student's *t*-test using GraphPad Prism 6 when the distribution was normal as revealed by the Kolmogorov–Smirnov test. If the distribution was not normal, mean fold-changes were analyzed with the Mann–Whitney test. Differences between groups were considered statistically significant at $*P < 0.05$, $**P < 0.01$, and $***P < 0.001$.

Protein extraction and western blotting

Thalamus samples (0.1 g) were homogenized using lysis buffer composed of 100 mM Tris pH 7, 100 mM NaCl, 10 mM EDTA, 0.5% NP-40 and 0.5% sodium deoxycholate plus protease and phosphatase inhibitors (Roche Molecular Systems, Pleasanton, CA, USA). Samples were centrifuged at 4°C for 5 minutes at 10,000 g USING Eppendorf centrifuge 5417R (Eppendorf®, Hamburg, Germany) and the supernatants obtained were stored at −80°C. Proteins were separated in sodium dodecylsulfate-polyacrylamide gel electrophoresis (SDS-PAGE). Control of protein loading was carried out with Coomassie blue staining. Proteins were then electrophoretically transferred to nitrocellulose membranes using the Trans-Blot® SD Semi-Dry Transfer Cell (Bio-Rad, Hercules, CA, USA) at 60 mA/membrane for 90 minutes). Nonspecific bindings were blocked by incubation in 5% milk in Tris-buffered saline (TBS) containing 0.2% Tween for 1 h at room temperature. After washing, the membranes were incubated at 4°C overnight with one of the primary antibodies listed in Table 3 in TBS containing 5% albumin and 0.2% Tween. Afterwards, the membranes were incubated for 1 h with the appropriate HRP-conjugated secondary antibody (1:1000, Dako, Glostrup, Denmark, Northern Europe), and the immune complexes were visualized with a chemiluminescence reagent (ECL, Amersham, GE Healthcare, Buckinghamshire, UK). Densitometry of western blot bands was assessed with the TotalLab program (TotalLab Quant, Newcastle, UK) and analyzed with Graphpad Prism using Student's *t*-test when the distribution was normal and Mann–Whitney test when the distribution was not normal, as assessed with the Kolmogorov–Smirnov normality test. Differences were considered statistically significant at $*P < 0.05$, $**P < 0.01$, and $***P < 0.001$.

Immunohistochemistry

Immunohistochemical study was performed in 4-μm thick dewaxed paraffin sections of the thalamus. Endogenous peroxidases were blocked with peroxidase (Dako, Glostrup) followed by 10% normal goat serum. The primary antibodies are shown in Table 3. Following incubation with the primary antibody at room temperature overnight, the sections were incubated with EnVision+ system peroxidase (Dako, Barcelona, Spain) at room temperature for 15 minutes. The peroxidise reaction was visualized with diaminobenzidine (DAB) and H_2O_2. No antigenic peptides were available to carry out preadsorption studies of primary antibodies. However, the omission of the primary antibody in some sections was used as a control of the immunostaining; no signal was obtained after incubation with only the secondary antibody. Sections were slightly counterstained with haematoxylin. Quantification of Nissl-stained and immunoreactive cells identified with antibodies against glial fibrillary acidic protein (GFAP), CD68, voltage-dependent anion channel (VDAC), nucleolin (NCL), nucleoplasmin 3 (NPM3), histone H3K9me2, ATP5H protein and superoxide dismutase 2 (SOD2) was carried out in the mediodorsal thalamus in five controls and five FFI cases (two fields per case) at a magnification of ×200 which corresponds to an area of 450 × 280 μm^2. Results were expressed as mean values ± standard deviation (SD).

RESULTS

General neuropathological findings

Severe neuronal loss and marked astrocytic gliosis was observed in every case in the mediodorsal and anterior nuclei of the thalamus, and inferior olives; the ventral nuclei of the thalamus and the entorhinal cortex were variably affected (five and six of seven cases, respectively). Spongiform change was not seen in the mediodorsal thalamus and only in the entorhinal cortex when affected PrP. Discrete astrogliosis was also found in the periaqueductal gray matter. Representative changes in the mediodorsal

Table 2. Abbreviated names of genes, their full names, and TaqMan probe references used for the study of mRNA expression of mitochondria, protein synthesis and purine metabolism enzymes including GUS-β and XPNPEP1 used for normalization.

Gene	Gene full name	Taqman probes
XPNPEP1	X-propylaminopeptidase 1	Hs00958026_m1
Mitochondria		
NDUFA2	NADH Dehydrogenase (ubiquinone) 1 apha subcomplex, 2, 8 kDa	Hs04187282_g1
NDUFA7	NADH dehydrogenase (ubiquinone) 1 alpha subcomplex, 7, 14.5 kDa	Hs01561430_m1
NDUFA10	NADH dehydrogenase (ubiquinone) 1 alpha subcomplex, 10, 42 kDa	Hs01071117_m1
NDUFB3	NADH Dehydrogenase (ubiquinone) 1 Beta subcomplex, 3, 12 kDa	Hs00991297_g1
NDUFB7	NADH Dehydrogenase (ubiquinone) 1 Beta subcomplex, 7, 18 kDa	Hs00188142_m1
NDUFB10	NADH dehydrogenase (ubiquinone) 1 beta subcomplex, 10, 22 kDa	Hs00605903_m1
NDUFS7	NADH dehydrogenase (ubiquinone) Fe-S protein 7, 20 kDa (NADH-coenzyme Q reductase)	Hs00257018_m1
NDUFS8	NADH dehydrogenase (ubiquinone) Fe-S protein 8, 23 kDa (NADH-coenzyme Q reductase)	Hs00159597_m1
SDHB	Succinate dehydrogenase complex, subunit B, Iron Sulfur (Ip)	Hs01042482_m1
UQCR11	Ubiquinol-cytochrome C reductase, complex III subunit XI	Hs00199138_m1
UQCRB	Ubiquinol-cytochrome C reductase binding protein	Hs01890823_s1
COX7A2L	Cytochrome c oxidase subunit VIIa polypeptide 2 like	Hs00190880_m1
COX7C	Cytochrome C oxidase subunit VIIc	Hs01595220_g1
ATP5D	ATP Synthase, H+ transporting, mitochondrial F1 complex, Delta Subunit	Hs00961521_m1
ATP5G2	ATP synthase, H+ transporting, mitochondrial Fo complex, subunit C2	Hs01086654_g1
ATP5H	ATP Synthase, H+ transporting, mitochondrial Fo complex, subunit D	Hs01046892_gH
ATP5L	ATP Synthase, H+ transporting, mitochondrial Fo complex, subunit G	Hs00538946_g1
ATP5O	ATP Synthase, H+ transporting, mitochondrial F1 complex, O subunit	Hs00426889_m1
ATP6V0B	ATPase, H+ transporting, lysosomal 21 kDa, V0 subunit b	Hs01072388_m1
ATP6V1H	ATPase, H+ transporting, lysosomal 50/57 kDa, V1 subunit H	Hs00977530_m1
TOMM40	Translocase of outer mitochondrial membrane 40	Hs01587378_mH
Protein synthesis		
NCL	Nucleolin	Hs01066668_m1
NPM1	Nucleophosmin/protein B23)	Hs02339479_g1
UBTF	Eukaryotic upstream binding factor	Hs01115792_g1
18S rRNA	Eukaryotic 18S rRNA	Hs99999991_s1
28S rRNA	RNA, 28S ribosomal	Hs03654441_s1
RPL5	Ribosomal protein L5	Hs03044958_g1
RPL7	Ribosomal protein L7	Hs02596927_g1
RPL21	Ribosomal protein L21	Hs00823333_s1
RPL22	Ribosomal protein L22	Hs01865331_s1
RPL23A	Ribosomal protein L23A	Hs01921329_g1
RPL26	Ribosomal protein L26	Hs00864008_m1
RPL27	Ribosomal protein L27	Hs03044961_g1
RPL30	Ribosomal protein L30	Hs00265497_m1
RPL31	Ribosomal protein L31	Hs01015497_g1
RPS3A	Ribosomal protein S3A	Hs00832893_sH
RPS5	Ribosomal protein S5	Hs00734849_g1
RPS6	Ribosomal protein S6	Hs04195024_g1
RPS10	Ribosomal protein S10	Hs01652370_gH
RPS13	Ribosomal protein S13	Hs01011487_g1
RPS16	Ribosomal protein S16	Hs01598516_g1
RPS17	Ribosomal protein S17	Hs00734303_g1
RPS20	Ribosomal protein S20	Hs00828752_gH

thalamus and entorhinal cortex compared with corresponding regions in age-matched controls are shown in Figure 1. Neuron loss in the mediodorsal thalamus was severe accounting for about 80%–90%; only isolated small neurons can be seen in some cases. Microglial response was analyzed using the antibodies Iba1 which identifies microglia and CD68 which recognizes active microglia. Increased numbers of Iba1- and CD68-immunoreactive cells was found in the mediodorsal thalamus, particularly in two of seven cases, and entorhinal cortex in the six cases in which this region was affected. Details of cell types are recognized at higher magnification (Figure 1 inserts)

Immunohistochemistry using the 3F4 antibody disclosed synaptic and fine granular proteinase-resistant PrP immunoreactivity in the entorhinal cortex, whereas PrP immunoreactivity was absent in the mediodorsal thalamus in FFI cases (Figure 2). As expected no proteinase-resistant PrP was present in control cases (data not shown).

Table 3. List of antibodies used for western blotting and immunohistochemistry.

Antibody	Reference	Supplier	Host	wb dilution	ihq dilution
Nucleolin	Ab22758	Abcam (Cambridge, UK)	rb	1/100	1/1000
Anti-eukaryotic translation initiation factor 2 (eIF2-α)	5A5	Thermo Scientific (Waltham, MA, USA)	m	1/50	
Anti-phospho-eIF2-alpha pSer51 (p-EIF2-α)	S.674.5	Thermo Scientific (Waltham, MA, USA)	rb	1/50	
Anti-eukaryotic translation initiation factor 5 (eIF5)	sc-282	Santa Cruz (Dallas, TX, USA)	rb	1/400	
Anti-eukaryotic elongation factor 1A (eEF1A)	2551	Cell signaling (Danvers, MA, USA)	rb	1/100	
Anti-eukaryotic elongation factor 2 (eEF2)	2332	Cell signaling (Danvers, MA, USA)	rb	1/500	
Total OXPHOS Antibody Cocktail	ab110411	Mitosciences, Abcam (Cambridge, UK)	m	1/1000	
ATP5O (OSCP antibody)	10994-1-AP	Proteintech (Chicago, IL, USA)	rb	1/1000	
UQCRB	10756-1-AP	Proteintech (Chicago, IL, USA)	rb	1/250	
VDAC1	Ab15895	Abcam (Cambridge, UK)	rb	1/400	1/100
β-actin	A5316	Sigma-Aldrich (St Louis, MO, USA)	m	1/5000	
ATP5H	17589-1-AP	Proteintech (Chicago, IL, USA)	rb		1/100
Anti-manganese superoxide dismutaseSOD2	SOD-110	Stressgen (San Diego, CA, USA)	rb		1/100
Anti-histone H3K9me2	Ab1220	Abcam (Cambridge, UK)	m		1/90

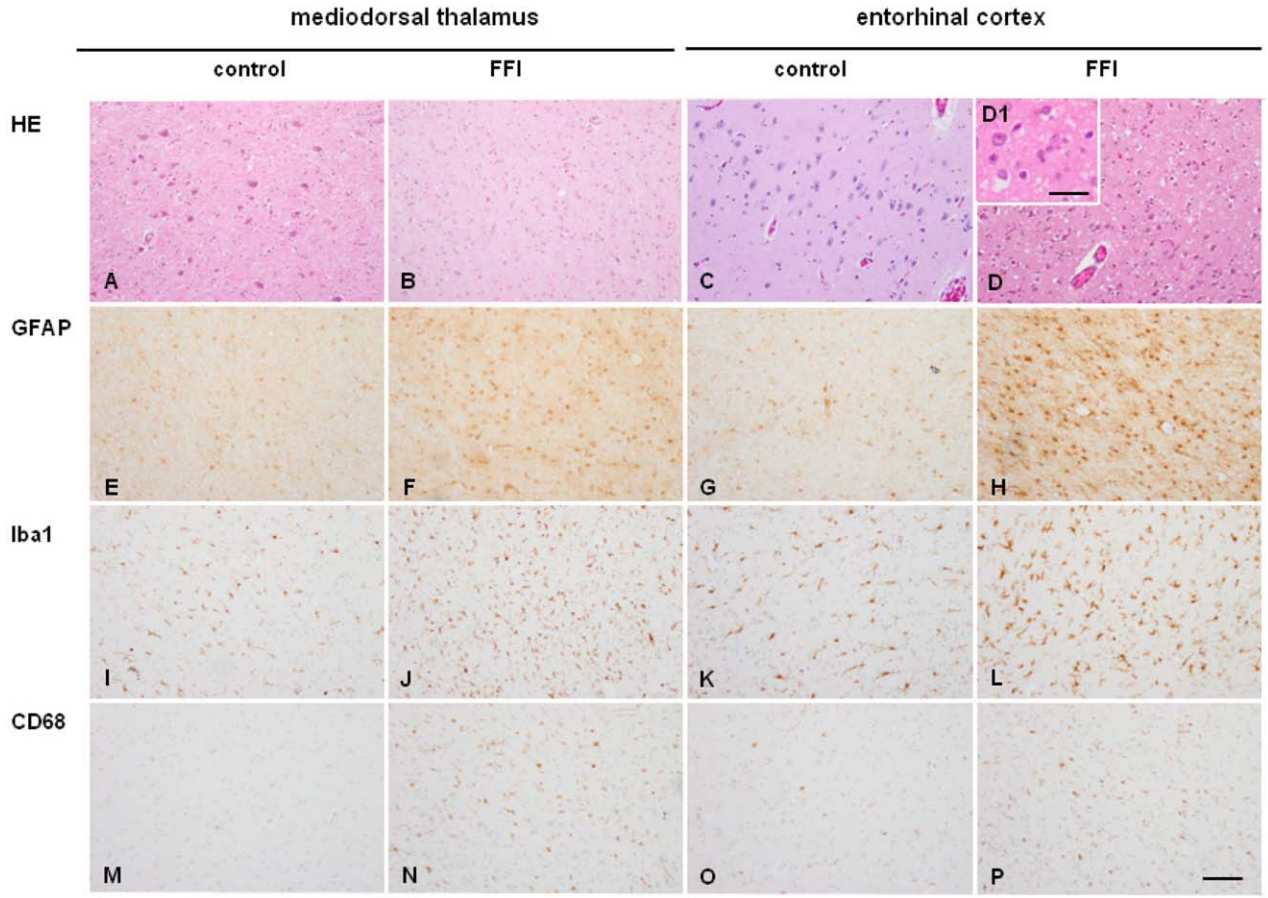

Figure 1. Mediodorsal thalamus (A, B, E, F, I, J, M, N) and entorhinal cortex C, D, G, H, K, L, O, P) in age-matched control (A, C, E, G, I, K, M, O) and FFI (B, D, F, H, J, L, N, P) cases. Severe neuron loss is seen in the mediodorsal thalamus in FFI, whereas moderate neuron loss and spongiform change is observed in the entorhinal cortex in FFI. Increased numbers of GFAP-immunoreactive astrocytes are present in mediodorsal thalamus and entorhinal cortex in FFI compared with corresponding controls. Increased numbers of Iba1-immunoreactive cells and CD-68-positive cells are seen in the EC in six cases and in two of seven FFI cases (here illustrated) compared with controls. Paraffin sections, **A–D.** haematoxylin and eosin; **E–H**. GFAP immunohistochemistry; **I–L**. Iba1 immunohistochemistry; **M–P.** CD-68 immunohistochemistry; immunohistochemical sections slightly counterstained with haematoxylin. A–P, bar in P = 55 μm. D1, H1, L1, P1, bar in P1 = 30 μm.

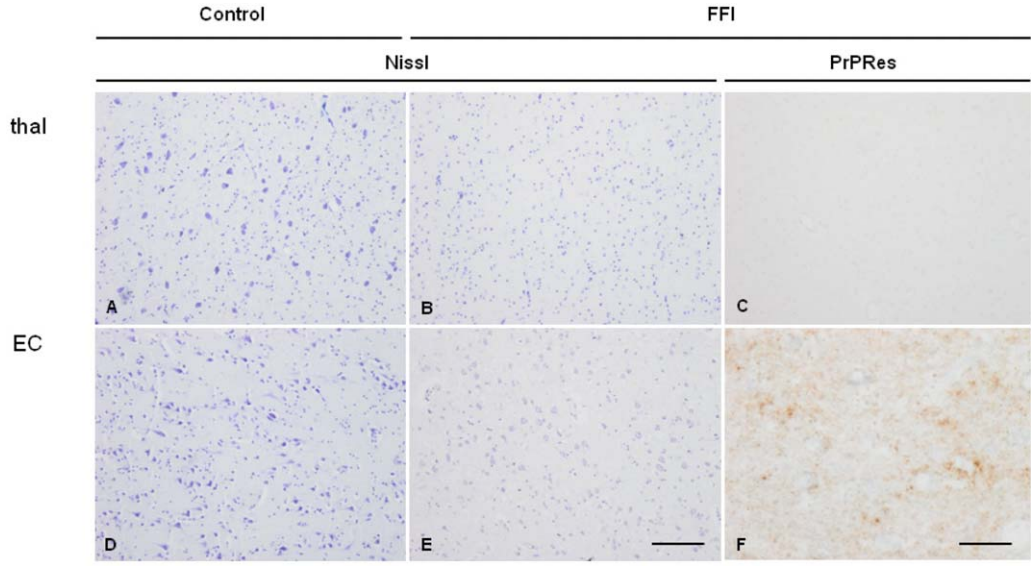

Figure 2. Mediodorsal nucleus of the thalamus (thal: **A–C**) and entorhinal cortex (EC: **D–F**) in control (A,B) and FFI (B,C,E,F) cases showing marked loss of neurons without spongiform change in the thalamus and moderate neuron loss and spongiform change in entorhinal cortex in FFI when compared with corresponding regions in controls. In FFI, no proteinase K-resistant PrP (PrPRes) is observed in the mediodorsal thalamus (C) whereas punctate, synaptic-like immunostaining is observed in the entorhinal cortex (F) processed in parallel. Paraffin sections, A, B, D, E Nissl staining, bar in E = 50 μm; C, F, PrP immunohistochemistry (3F4 antibody) following preincubation with proteinase K, bar in F = 25 μm.

Mitochondria and respiratory chain

mRNA expression

Eleven genes which codify for proteins that are part of electron transport chain complexes, one gene that encodes a translocase of the mitochondrial outer membrane (*TOMM40*) and two genes that codify for lysosomal ATPase (*ATP6V0B* and *ATP6V1H1*) were analyzed in the thalamus of FFI samples. Complex I was represented by *NDUFA2*, *NDUFA7*, *NDUFA10*, *NDUFB3*, *NDUFB7*, *NDUFB10*, *NDUFS7*, and *NDUFS8*; complex II by *SDHB*; complex III by *UQCR11* and *UQCRB*; complex IV by *COX7A2L* and *COX7C*; and complex V by *ATP5D*, *ATP5G2*, *ATP5H*, *ATP5L*, and *ATP5O*. Only *ATP5D* was downregulated (Student's *t*-test $P < 0.01$). Detailed data are shown in Supporting Information Table S1.

Protein expression of selected mitochondrial proteins

Expression levels of mitochondrial proteins in mediodorsal thalamus. NDUFB8 (complex I subunit), SDHB (complex II subunit), UQCRC2 (complex III subunit), COX2 (complex IV subunit), and ATP50 (complex V) expression levels, as revealed by western blotting, were reduced in mediodorsal thalamus in FFI, whereas UQCRB (complex III) and ATP5A (complex V subunit) expression was similar in FFI and controls. Densitometric analysis using β-actin and VDAC for normalization showed similar results, the only exception between β-actin and VDAC normalization was ATP5O which presented significant differences when using β-actin between control group and FFI group but only a tendency with a *P*-value 0.09 when using VDAC for normalization. Together, these results indicated that reduced protein expression of proteins of the respiratory chain was not merely the consequence of a reduced number of mitochondria, but was also related to the selective loss of certain vulnerable subunits (Figure 3). Detailed data are shown in Supporting Information Table S2.

VDAC, ATP5H, and SOD2 in mediodorsal thalamus in FFI. Consecutive sections were stained with Nissl staining and processed for immunohistochemistry to VDAC, ATP5H, and SOD2. Nissl staining served to illustrate the severe loss of neurons in the mediodorsal thalamus in FFI when compared with controls, together with the increase in the number of small nuclei corresponding, in part to astrocytes (Figures 4A,B).

In control brains, neurons presented strong VDAC immunoreactivity, punctuate ATP5H immunoreactivity and weak SOD2 immunoreactivity in the cytoplasm. Marked decrease in VDAC immunoreactivity related to the loss of neurons was observed in the mediodorsal thalamus in FFI when compared with controls (Figures 4C,D). This was accompanied by general decrease in ATP5H immunoreactivity due to neuron loss together with enhanced visualization of ATP5H immunostaining in reactive astrocytes (Figures 4E,F). Marked SOD2 immunoreactivity was found in reactive astrocytes (Figures 4G,H). Details of cell types are recognized at higher magnification (Figure 4 inserts). Quantitative data are shown in Table 4.

MOLECULAR PATHWAYS INVOLVED IN PROTEIN SYNTHESIS

mRNA expression of ribosomal proteins RPL and RPS, nucleolar proteins, and 18S rRNA and 28S rRNA

Nucleolin (*NCL*), nucleophosmin (*NPM1*), and eukaryotic upstream binding factor (*UBTF*) gene expression levels were

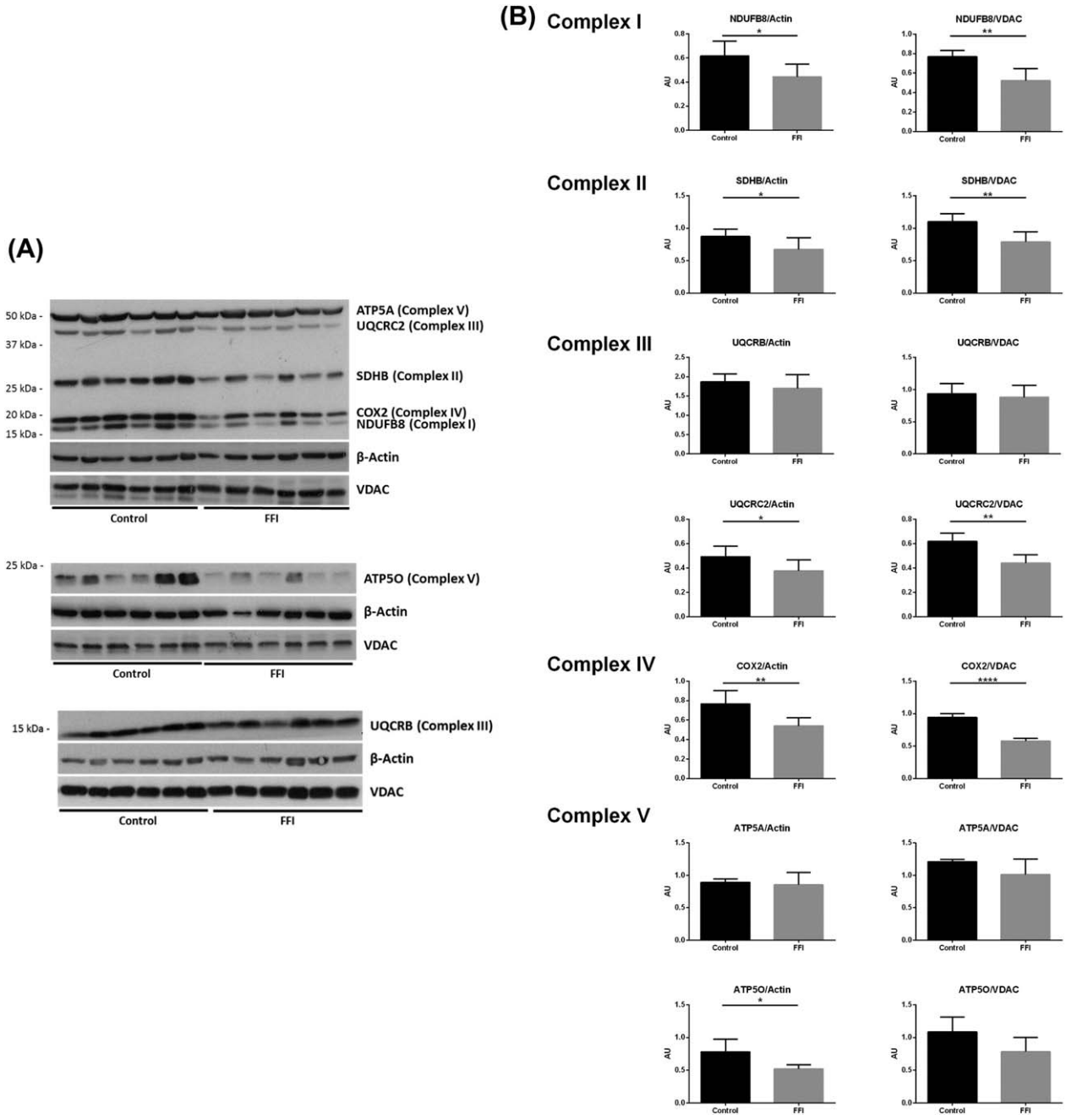

Figure 3. A. Western blot of subunits NADH dehydrogenase (ubiquinone) 1 beta subcomplex 8, 19 kDa (NDUFB8), succinate dehydrogenase complex, subunit B, iron sulphur (Ip) (SDHB), ubiquinol-cytochrome c reductase core protein II (UQCRC2), cytochrome c oxidase subunit II (COX2) and ATP synthase, H+ transporting, mitochondrial F1 complex, and alpha subunit 1 (ATP5A) using OXPHOS antibody; ATP synthase, H+ transporting mitochondrial F1 complex, O subunit (ATP5O) and ubiquinol-cytochrome c reductase binding protein (UQCRB) antibodies in mediodorsal thalamus in FFI and control cases. β-actin and VDAC were used to normalize total protein and mitochondria protein loading, respectively. **B.** Densitometric analysis shows significant reduction of NDUFB8, SDHB, UQCRC2, and COX2 normalized with β-actin and VDAC in FFI compared with controls. ATP5A and UQCRB protein levels were preserved. Results were analyzed by Graphpad Prism with Student's *t*-test when the distribution was normal and with Mann–Whitney test if distribution was not normal as assessed with the Kolmogorov–Smirnov normality test. Differences are considered statistically significant at $^{*}P<0.05$, $^{**}P<0.01$, and $^{****}P<0.0001$. ATP5O shows a significant reduction when normalized with β-actin but only a trend with VDAC.

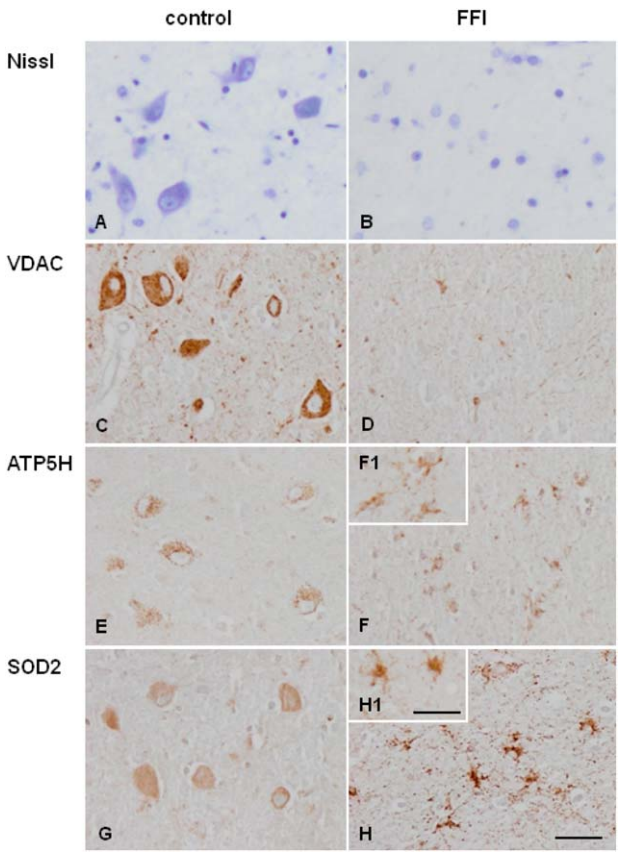

Figure 4. Mediodorsal nucleus of the thalamus in control (**A, C, E, F**) and FFI (**B, D, F, H**) cases. Nissl staining (A, B) shows marked decrease in the number of neurons in FFI when compared with controls. (VDAC) (C, D), (C, D) (SOD2) (E, F) immunoreactivity is found in mediodorsal thalamus in control (A, C, E) and FFI (B, D, F) cases). Decreased VDAC (C, D) and ATP synthase, H+ transporting, mitochondrial Fo complex, subunit d (ATP5H) (E, F) immunoreactivity is found in the mediodorsal thalamus in FFI compared with controls due to the dramatic decrease in the number of neurons. However, ATP5H is observed in reactive glial cells. Weak superoxide dismutase 2 (SOD2) (G, H) immunoreactivity is seen in neurons in control cases which contrasts with enhanced SOD2 immunostaining in reactive astrocytes in FFI. Paraffin sections, A, B: Nissl staining; C–H immunohistochemical sections slightly counterstained with haematoxylin. A–H, bar in H = 25 μm. F1, H1, bar in H1 = 10 μm.

analyzed in FFI cases and controls. *NPM1* was upregulated in the thalamus in FFI (Figure 5).

28S rRNA was also upregulated in FFI cases (Figure 5).

The expression of nine RPL (*RPL5*, *RPL7*, *RPL21*, *RPL22*, *RPL23A*, *RPL26*, *RPL27*, *RPL30*, and *RPL31*) and seven RPS (*RPS3A*, *RPS5*, *RPS6*, *RPS10*, *RPS13*, *RPS17*, and *RPS20*) genes was assessed in the mediodorsal thalamus in FFI cases and controls. *RPS17* and *RPS20* were upregulated (Figure 5). Detailed data are shown in Supporting Information Table S3.

Immunohistochemistry of selected molecules involved in protein synthesis

In control mediodorsal thalamus, anti-NCL antibodies weakly decorated the nucleolus and heavily the cytoplasm of neurons. NCL immunoreactivity was weak if present in glial cells under the same staining conditions. Anti-nucleoplasmin 3 (NPM3) antibodies decorated the nucleolus of neurons. Histone H3 di-methylated K9 (H3K9me2), which modulates NCL and NPMs function in rRNA transcription (4, 35), was strongly expressed in the nucleus of neurons (Figures 6A,C,E).

Immunoreactivity of NCL and (NPM3) was reduced in the mediodorsal thalamus in FFI cases when compared with controls (Figures 6B,D). H3K9me2 expression was also decreased in the thalamus in FFI (Figure 6F). NCL, NPM3, and H3K9me2 reduction in the mediodorsal thalamus was clearly due to the loss of neurons; reactive glial cells (already represented in previous figures) did not show increased immunoreactivity. Quantitative data are shown in Table 4.

Table 4. Quantitative data of cells stained with Nissl stain and immunoreactive with antibodies against voltage-dependent anion channel (VDAC), glial fibrillary acidic protein (GFAP), CD8 (reactive microglia), nucleolin (NCL), nucleoplasmin 3 (NPM3), histone H3K9me2, ATP5H protein and superoxide dismutase 2 (SOD2) in the mediodorsal thalamus in control and FFI cases. Values are expressed as mean values ± SD. Assessed cell types are named in the left column excepting ATP5H and SOD2 immunoreactive cells which are neurons in controls and glia in FFI cases.

	Control	FFI
Nissl (only neurons)	20.5 ± 2.01	0.9 ± 073
VDAC (only neurons)	20.4 ± 2.06	1.3 ± 0.94
GFAP (astrocytes)	8.8 ± 2.09	35 ± 6.87
CD68 (reactive microglia)	2.3 ± 0.94	18.4 ± 3.40
NCL (only neurons	6.8 ± 1.81	0
NPM3 (only neurons)	6 ± 1.82	0
H3K9me2 (only neurons)	21.8 ± 2.04	0
ATP5H	23.7 ± 2.45 (neurons)	23 ± 3.52 (glia)
SOD2	20.6 ± 1.83 (neurons)	25.5 ± 2.83 (glia)

Expression of nucleolin, and initiation and elongation factors, in mediodorsal thalamus

Expression levels of nucleolin were markedly decreased in the mediodorsal thalamus in FFI (Figure 7) as expected from the immunohistochemical studies. Regarding initiation and elongation factors, only eEF1A was significantly decreased in the mediodorsal thalamus of FFI cases (Figure 7). Detailed data are shown in Supporting Information Table S4.

DISCUSSION

All the cases examined in the present series are males, have the D178N mutation and are Met/Met homozygous at the codon 129 of *PRNP*. In spite of the variable age at onset, disease duration was between 6 and 9 months; the neuropathological findings were similar from one case to another; therefore, this series conforms a relative homogeneous population. General neuropathological findings in these series are similar to those already described in FFI (14, 21, 22, 26, 28). Based on these features and on the small number of cases, no attempt was made to divide the sample into subgroups.

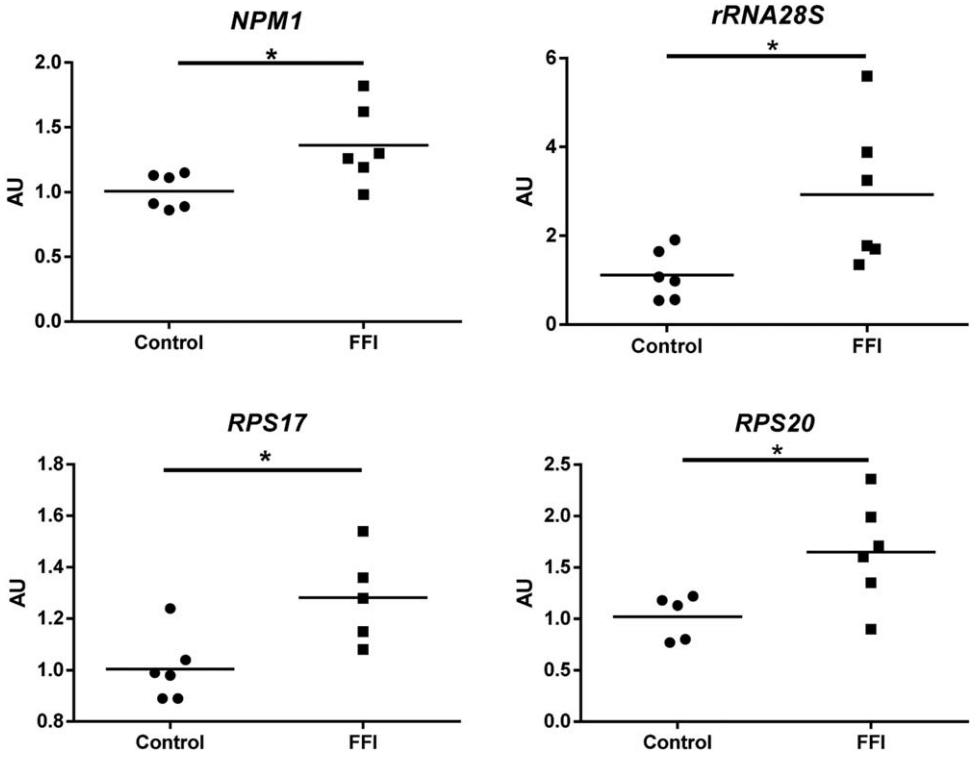

Figure 5. mRNA expression of ribosomal proteins (RPL and RPS) in mediodorsal thalamus in FFI and controls. *RPS17*, *RPS20*, *NMP1*, and *28S rRNA* are upregulated in FFI cases using *XPNPEP1* for normalization. Mean fold-change values for each group are compared with Student's *t*-test and differences were considered statistically significant at $*P < 0.05$.

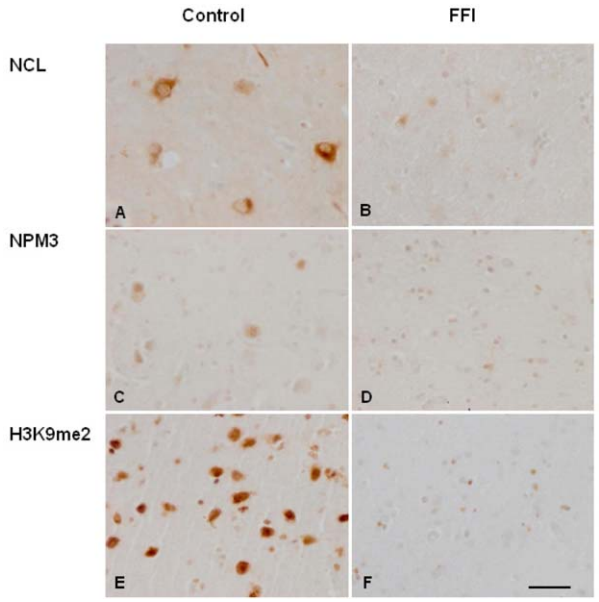

Figure 6. Nucleolin (NCL) (**A, B**), NPM3 (**C, D**), and H3 dimethyl K9 (H3K9me2) (**E, F**) immunoreactivity is observed in neurons in the mediodorsal thalamus in controls (A, C, E). Weak NCL immunoreactivity is found in the nucleolus whereas strong NCL immunoreactivity is present in the neuronal cytoplasm. NPM3 immunoreactivity is observed in the nucleolus, whereas H3K9me2 immunolabeling is localized in the nucleus. Decreased NCL, NMP3, and H3K9me2 expression is found in FFI cases (B, D, E) due to the marked decrease in the number of neurons. Paraffin sections slightly counterstained with haematoxylin; bar = 25 μm.

The postmortem delay between death and processing was longer in the FFI group when compared with the controls. However, the RIN values were similar in both groups and protein preservation as revealed by western blotting and immunohistochemistry was similar in controls and diseased brains.

Brain hypo-metabolism, as revealed by [18F]-2-fluoro-2-deoxy-D-glucose and positron emission tomography PET to study regional cerebral glucose utilization, predominates in the thalamus and cingular cortex, but the basal and lateral frontal cortex, the caudate nucleus, and the middle and inferior temporal cortex are also moderately affected (7). The neurodegenerative process starts between 13 and 21 months before the clinical symptoms and it is manifested by hypo-metabolism in the thalamus and impaired thalamic sleep spindle formation in preclinically affected family members (6). The present findings are in line with functional studies showing down-regulation of *ATP5D* mRNA expression as revealed by qRT-PCR, and significant reduction in the expression of NDUFB8 (complex I subunit), SDHB (complex II subunit), UQCRC2 (complex III subunit), COX2 (complex IV subunit), and ATP5O (complex V subunit) protein levels, as assessed with western blotting of total homogenates of the mediodorsal thalamus. Immunohistochemistry discloses the origin of reduced mitochondrial expression as being linked to severe neuron loss, as practically no neurons were stained with antibodies against VDAC and ATP5H. These changes are accompanied by increased oxidative stress responses manifested by increased SOD2 immunostaining in reactive astrocytes.

The expression of molecules involved in the machinery of protein synthesis was also altered in the mediodorsal thalamus in FFI when compared with controls. Curiously, increased mRNA

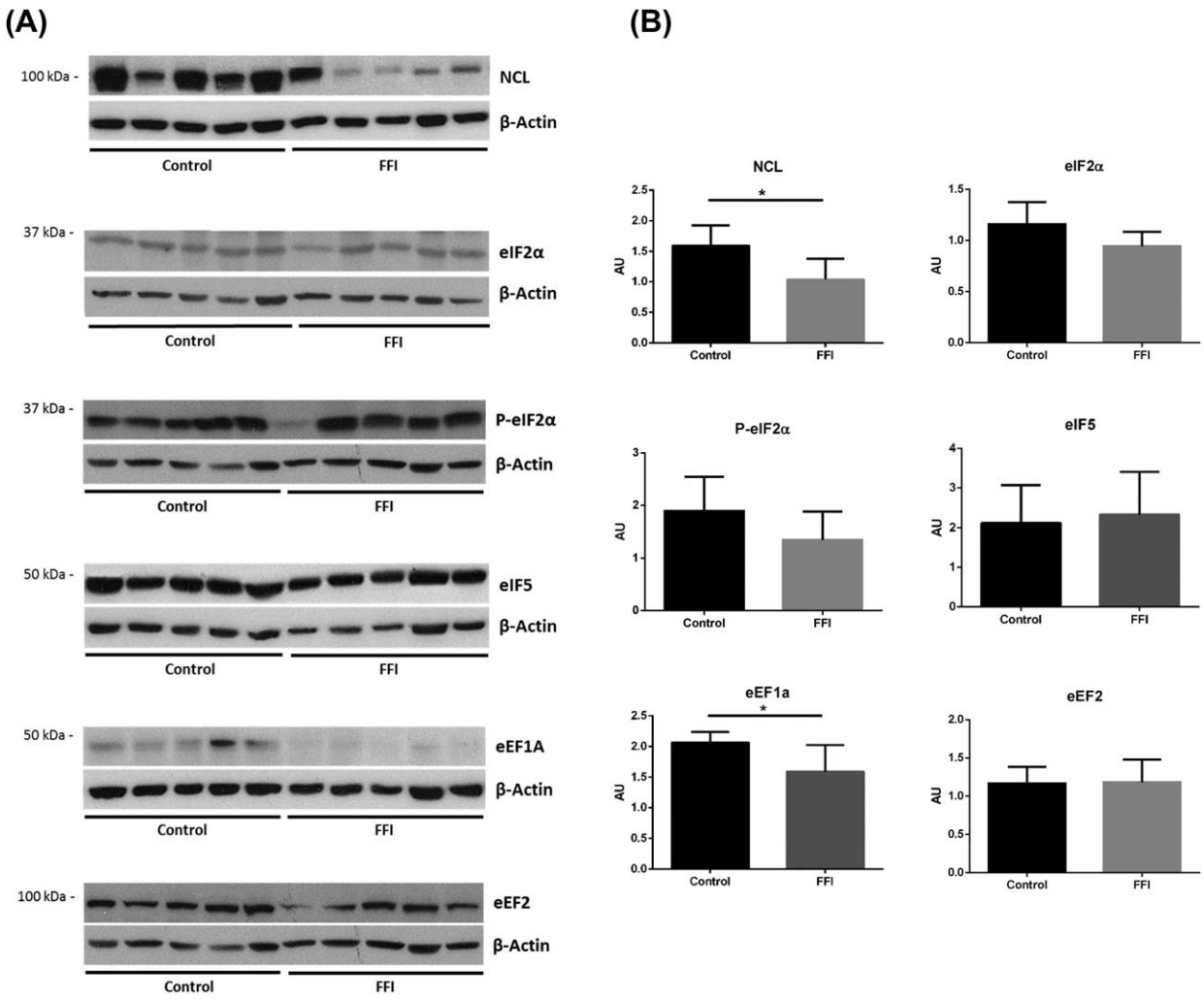

Figure 7. A. Western blots of nucleolin, initiation (eIF2α, P-eIF2α, eIF5) and elongation factors (eEF1A, eEF2) in mediodorsal thalamus in FFI and control cases. β-actin was used to normalize total protein. **B**. Densitometric analysis shows significant reduction of NCL and eEF1A. Results were analyzed by Graphpad Prism with Student's *t*-test when the distribution was normal and with Mann–Whitney test if distribution was not normal as assessed with the Kolmogorov–Smirnov normality test. Differences are considered statistically significant at $^*P < 0.05$.

expression of *NPM1*, 28S rRNA, *RPS17*, and *RPS20* is in contrast to the decreased protein expression levels of the histone-binding chaperones nucleolin (NCL) and nucleoplasmin 3 (NPM3), which regulate rRNA transcription (2, 4, 10, 11, 16, 18, 27), and of histone H3 di-methylated K9 (H3K9me2), which modulates NCL and NPMs function in rRNA transcription (4, 35). Changes in protein expression are clearly related to the dramatic reduction of neurons as disclosed by immunohistochemistry.

Regarding the protein expression of initiation and elongation factors of protein transcription, only eEF1A is downregulated. However, the role of this factor is crucial, as elongation occurs when eEF1A is activated following GTP binding and forms a complex with aminoacyl-tRNA, which recognizes the specific sequence in mRNA at the ribosome. Once the interaction of the codon in mRNA with the anti-codon in tRNA is decoded, eEF1A-GDP is hydrolyzed, released from the ribosome, and recycled into its active form by eEF1B. eEF2 assists in the precise codon location at the ribosome (1, 8, 32, 38).

Present molecular studies show reduced expression of proteins linked to the mitochondrial respiratory chain involving subunits encoded by genomic DNA of the five mitochondrial complexes in line with a marked reduction in the number of neurons as revealed by morphological and immunohistochemical studies, as well as decreased metabolism as shown by PET studies *in vivo* in the mediodorsal nucleus of the thalamus in FFI. Altered machinery of protein synthesis is also manifested by decreased expression of nucleolar chaperones, histone modifications and decreased methylation of DNA in the mediodorsal thalamus in FFI. Alterations in the levels of proteins do not correlate with modifications in the expression of corresponding mRNA levels, which are often maintained or even upregulated. This may be explained by failed compensatory mechanisms in the remaining neurons or by increased RNA expression in reactive astrocytes. In favor of the latter, is the dramatic increase in reactive astrocytes and the increased expression of superoxide dismutase 2 which tags reactive astrocytes as crucial components of oxidative stress responses in the mediodorsal thalamus in FFI.

All these changes are observed at terminal stages of the disease, with devastating effects on selected brain regions. Little can be done at this stage but efforts must be made at preclinical stages to prevent mitochondrial and protein synthesis havoc at advanced stages of the disease.

ACKNOWLEDGMENTS

This study was funded by the Ministerio de Ciencia e Innovación, Instituto de Salud Carlos III – Fondos FEDER, a Way to Build Europe FIS grant PI14/00757, and coordinated Intraciber 2014. We wish to thank T. Yohannan for editorial help.

REFERENCES

1. Andersen GR, Nissen P, Nyborg J (2003) Elongation factors in protein biosynthesis. *Trends Biochem Sci* **28**:434–441.
2. Angelov D, Bondarenko VA, Almagro S, Menoni H, Mongelard F, Hans F *et al* (2006) Nucleolin is a histone chaperone with FACT like activity and assists remodeling of nucleosomes. *EMBO J* **25**:1669–1679.
3. Capellari S, Strammiello R, Saverioni D, Krtezschmar H, Parchi P (2011) Genetic Creutzfeldt-Jakob disease and fatal familial insomnia: insights into phenotypic variability and disease pathogenesis. *Acta Neuropathol* **121**:21–37.
4. Cong R, Das S, Ugrinova I, Kumar S, Mongerlard F, Wong J, Bouvet P (2012) Interaction of nucleolin with ribosomal RNA genes and its role in RNA polymerase I transcription. *Nucleic Acids Res* **40**:9441–9454.
5. Cortelli P, Gambetti P, Montagna P, Lugaresi E (1999) Fatal familial insomnia: clinical features and molecular genetics. *J Sleep Res* **8**:23–29.
6. Cortelli P, Perani D, Montagna P, Gallassi R, Tinuper P, Federica P *et al* (2006) Pre-symptomatic diagnosis in fatal familial insomnia: serial neurophysiological and 18FDG-PET studies. *Brain* **129**: 668–675.
7. Cortelli P, Perani D, Parchi P, Grassi F, Montagna P, De Martin M *et al* (1997) Cerebral metabolism in fatal familial insomnia: relation to duration, neuropathology, and distribution of protease-resistant prion protein. *Neurology* **49**:126–133.
8. Dever TE, Green R (2012) The elongation, termination, and recycling phases of translation in eukaryotes. *Cold Spring Harb Perspect Biol* **4**: a013706.
9. Durrenberger PF, Fernando FS, Magliozzi R, Kashefi SN, Bonnert TP, Ferrer I *et al* (2012) Selection of novel reference genes for use in the human central nervous system: a BrainNet Europe study. *Acta Neuropathol* **124**:893–903.
10. Frehlick LJ, Eirín-López JM, Ausio J (2007) New insights into the nucleophosmin/nucleoplasmin family of nuclear chaperones. *Bioassays* **29**:49–59.
11. Gadad SS, Shandilya J, Kishore AH, Kundu TK (2010) NPM3, a member of the nucleophosmin/nucleoplasmin family, enhances activator-dependent transcription. *Biochemistry* **49**:1355–1357.
12. Gallassi R, Morreale A, Montagna P, Cortelli P, Avoni P, Castellani R *et al* (1996) Fatal familial insomnia: behavioral and cognitive features. *Neurology* **46**:935–939.
13. Gambetti P, Parchi P, Chen SG (2003) Hereditary Creutzfeldt-Jakob disease and fatal familial insomnia. *Clin Lab Med* **23**:43–64.
14. Gambetti P, Parchi P, Petersen RB, Chen SG, Lugaresi E (1995) Fatal familial insomnia and familial Creutzfeldt-Jakob disease: clinical, pathological and molecular features. *Brain Pathol* **5**:43–51.
15. Goldfarb LG, Petersen RB, Tabaton M, Brown P, LeBlanc AC, Montagna P *et al* (1992) Fatal familial insomnia and familial Creutzfeldt-Jakob disease: disease phenotype determined by a DNA polymorphism. *Science* **258**:806–808.
16. Huang N, Negi S, Szebeni A, Olson MOJ (2005) Protein NPM3 interacts with the multifunctional nucleolar protein B23/nucleophosmin and inhibits ribosome biogenesis. *J Biol Chem* **280**:5496–5502.
17. Krasnianski A, Bartl M, Sanchez Juan PJ, Heinemann U, Meissner B, Varges D *et al* (2008) Fatal familial insomnia: clinical features and early identification. *Ann Neurol* **63**:658–661.
18. Lindström MS (2011) NPM1/B23: a multifunctional chaperone in ribosome biogenesis and chromatin remodeling. *Biochem Res Int* 195209.
19. Livak KJ, Schmittgen TD (2001) Analysis of relative gene expression data using real-time quantitative PCR and the 2(-Delta Delta C(T)) method. *Methods* **25**:402–408.
20. Lugaresi A, Baruzzi A, Cacciari E, Cortelli P, Medori R, Montagna P *et al* (1987) Lack of vegetative and endocrine circadian rhythms in fatal familial thalamic degeneration. *Clin Endocrinol (Oxf)* **26**:573–580.
21. Lugaresi E, Medori R, Montagna P, Baruzzi A, Cortelli P, Lugaresi A *et al* (1986) Fatal familial insomnia and dysautonomia with selective degeneration of thalamic nuclei. *N Engl J Med* **315**:997–1003.
22. Manetto V, Medori R, Cortelli P, Montagna P, Tinuper P, Baruzzi A *et al* (1992) Fatal familial insomnia: clinical and pathologic study of five new cases. *Neurology* **42**:312–319.
23. Medori R, Tritschler HJ (1993) Prion protein gene analysis in three kindred with fatal familial insomnia (FFI): codon 178 mutation and codon 129 polymorphism. *Am J Hum Genet* **53**:822–827.
24. Medori R, Tritschler HJ, LeBlanc A, Villare F, Manetto V, Chen HY *et al* (1992) Fatal familial insomnia, a prion disease with a mutation at codon 178 of the prion protein gene. *N Engl J Med* **326**:444–449.
25. Monari L, Chen SG, Brown P, Parchi P, Petersen RB, Mikol J *et al* (1994) Fatal familial insomnia and familial Creutzfeldt-Jakob disease: different prion proteins determined by a DNA polymorphism. *Proc Natl Acad Sci U S A* **91**:2839–2842.
26. Montagna P, Gambetti P, Cortellui P, Lugaresi E (2003) Familial and sporadic fatal insomnia. *Lancet Neurol* **2**:167–176.
27. Okuwaki M, Matsumoto K, Tsujimoto M, Nagata K (2011) Function of nucleoplasmin/B23, a nucleolar acidic protein, as a histone chaperone. *FEBS Lett* **506**:272–276.
28. Parchi P, Capellari S, Gambetti P (2011) Fatal familial and sporadic insomnia. In: *Neurodegeneration: The Molecular Pathology of Dementia and Movement Disorders*. DW Dickson, RO Weller (eds), pp. 346–349. Wiley-Blackwell: Oxford.
29. Parchi P, Castellani R, Cortelli P, Montagna P, Chen SG, Petersen RB *et al* (1995) Regional distribution of protease-resistant prion protein in fatal familial insomnia. *Ann Neurol* **38**:21–29.
30. Parchi P, Petersen RB, Chen SG, Autilio-Gambetti L, Capellari S, Monari L *et al* (1998) Molecular pathology of fatal familial insomnia. *Brain Pathol* **8**:539–548.
31. Rodriguez-Martinez AB, Alfonso-Sanchez MA, Peña JA, Sanchez-Valle R, Zerr I, Capellari S *et al* (2008) Molecular evidence of founder effects of fatal familial through SNP haplotypes around the D178N mutation. *Neurogenetics* **9**:109–118.
32. Sasikumar AN, Perez WB, Kinzy TG (2012) The many roles of the eukaryotic elongation factor 1 complex. *Wiley Interdiscip Rev RNA* **3**: 543–555.
33. Schroeder A, Mueller O, Stocker S, Salowsky R, Leiber M, Gassmann M *et al* (2006) The RIN: an RNA integrity number for assigning integrity values to RNA measurements. *BMC Mol Biol* **7**:3.
34. Shi Q, Chen LN, Zhang BY, Xiao K, Zhou W, Chen C *et al* (2015) Proteomics analyses for the global proteins in the brain tissues of different human prion diseases. *Mol Cell Proteomics* **14**:854–869.
35. Tamada H, Thuan NV, Reed P, Nelson D, Katoku-Kikyo N, Wudel J *et al* (2006) Chromatin decondensation and nuclear reprogramming by nucleoplasmin. *Mol Cell Biol* **26**:1259–1271.
36. Tian C, Liu D, Sun Q-L, Chen C, Xu Y, Wang H *et al* (2013) Comparative analysis of gene expression profiles between cortex and

thalamus in Chinese fatal familial insomnia patients. *Mol Neurobiol* **48**:36–48.
37. Tinuper P, Montagna P, Medori R, Cortelli P, Zucconi M, Baruzzi A, Lugaresi E (1989) The thalamus participates in the regulation of sleep-waking cycle. A clinic-pathological study in fatal familial thalamic degeneration. *Electroencephalogr Clin Neurophysiol* **73**:117–123.
38. Voorhees RM, Ramakrishnan V (2013) Structural basis of the translational elongation cycle. *Annu Rev Biochem* **82**:203–236.

SUPPORTING INFORMATION

Additional Supporting Information may be found in the online version of this article at the publisher's web-site.

Table S1. Gene expression of subunits of mitochondrial complexes in the mediodorsal thalamus in FFI and control cases normalized with XPNPEP1.
Table S2. Densitometric values of expression of mitochondrial proteins as revealed by western blotting in the mediodorsal thalamus in FFI cases and controls normalized with β-actin (A) and VDAC (B).
Table S3. Gene expression of nucleolar proteins. 18S and 28S rRNAS and ribosomal proteins in the mediodorsal thalamus in FFI and control cases normalized with XPNPEP1.
Table S4. Densitometric values of expression of initiation and elongation factors of protein transcription in the mediodorsal thalamus in FFI cases and controls normalized with β-actin.